euspen's 24th International Conference & Exhibition, Dublin, IE, June 2024
www.euspen.eu

Modelling and control of turbine-driven spindles for micro machining with constant feed per tooth

Andreas Lange[1], Nicolas Altherr [1], Felix Zell[1], Benjamin Kirsch[1], Jan C. Aurich[1]

[1]*RPTU Kaiserslautern; Institute for Manufacturing Technology and Production Systems*

felix.zell@rptu.de

Abstract

Micro machining requires high spindle speeds but only needs low cutting power, making turbines a potential alternative to electric motors. As an increased surface quality and tool life can be achieved through a constant feed per tooth when using micro end mills, it is necessary to adapt the spindle speed to the feed rate alteration. Hence, the drive's dynamics and torque must be sufficient to ensure fast adaptions of the spindle speed to the feed rate alteration, which is more difficult with turbines.
This paper aims to model a speed control system for turbine-driven spindles, examining the suitability of a turbine's dynamics and torque to adapt the spindle speed to feed rate alterations. The modelling approach consists of three stages: 1. Setup of a fluid dynamics simulation to determine torque across various inlet mass flow rates and generating lookup tables for later control system implementation. 2. Designing a controller featuring a feedback loop with feedforward control for fast adaptation and accurate control of model uncertainties and disturbances. 3. Integrating the turbine's flow dynamics and rotor's dynamics into the feedback loop.
The evaluation of the control behaviour shows that effective control can be achieved. Hence, the devised control concept theoretically enables fast speed adjustments. However, the turbine's torque is not high enough to enable the required fast changes of the rotational speed to maintain a constant feed per tooth. A higher mass flow rate could generate sufficient torque, as shown by artificially increasing the mass flow rate, but it was not possible to increase the mass flow rate further with the chosen geometry and fluid dynamics boundary conditions. Turbine optimization could increase torque but might necessitate trade-offs between added rotor inertia and improved torque. Additionally, the employed turbines exhibit lower efficiency compared to electric motors.

Micromachining, Simulation, Turbine blade, Control

1. Introduction

Micro machining is crucial for manufacturing high-precision and complex microstructures [1, 2]. In micro machining processes such as micro milling, it is desirable to employ a constant optimal feed per tooth, as this can significantly influence the process result and reduce tool wear [2, 3]. As such, the spindle speed must be adapted to the feed rate to maintain a constant feed per tooth, which requires sufficient spindle torque and dynamics to enable fast speed control.

High-frequency spindles used for micro machining are usually driven by electric motors [4], but this generates electromagnetic fields that can affect the run-out [5]. An alternative drive method is a turbine, which has no electromagnetic fields. Further, high-frequency spindles are often equipped with air bearings [6], which enables the use of compressed air for both the bearings and the turbine. In addition, turbines generate less heat than electric motors, which improves the thermal stability of the spindle-system [7]. Disadvantage of turbines in high-frequency spindles are their low efficiency, power output, and dynamics, as previous works have shown [8].

In this study, a speed control of a spindle's turbine drive is developed. For this purpose, the control loop is modelled, including the flow dynamics of the turbine. Further, the cutting torque is considered. The turbine is modelled via a numerical fluid dynamics model, which is implemented in the control loop in the form of lookup tables to enable efficient access to the required mass-flow-rate-speed-torque characteristics of the turbine. A compensation controller is designed using root locus analysis.

2. Methods

First, the fluid dynamics simulation is conducted to determine the mass-flow-rate-speed-torque characteristics of the turbine. Next, the kinematics for micro milling a groove with constant feed per tooth are described, as needed for defining the requirements for the speed control to keep a constant feed per tooth. Subsequently, the feedback loop and controller are modelled.

2.1. Fluid dynamics simulation

To determine the mass-flow-rate-speed-torque characteristics of the turbine, a fluid dynamics simulation was conducted, describing the behaviour of the fluid volume (air) between the turbine and the casing. In Figure 1a), the CAD model of the rotor is depicted, consisting of a single axial and two radial bearing surfaces and two turbine geometries with eight semi-circular blades each. Two turbines with blades facing opposite directions are required for fast acceleration and deceleration. At the front end of the rotor, the micro milling tool can be mounted. Figure 1b) shows the CAD model of the fluid volume. The CAD model of the fluid volume was imported into ANSYS[1] Fluent[1] for computation of the resulting torque.

The simulation requires boundary conditions defining external influences on the flow. In this case, the boundary conditions include mass flow rate at the inlet, rotor speed, and ambient pressure at the outlet. The simulation was performed for four different combinations of mass flow rate and rotor speed. For each combination, the resulting turbine torque was computed. Only four combinations were simulated because the torque is linearly

dependent on both the rotor speed and mass flow rate. Thus, four combinations/result points are sufficient to describe the characteristics.

The mass-flow-rate-speed-torque characteristics of the turbine were derived from the fluid dynamics simulation results by fitting a plane through the four result points using linear regression. The resulting values were stored in lookup-tables for the implementation in the feedback loop. The Curve Fitter App[1] in MATLAB[1] was employed for linear regression.

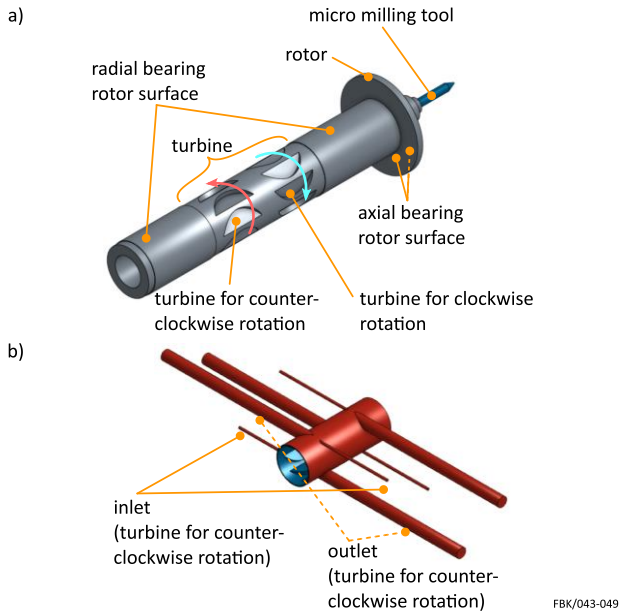

Figure 1. a) schematic view of the spindle rotor with incorporated turbines, b) modelled fluid region and boundary conditions

2.2. Requirements to enable constant feed per tooth

To keep the feed per tooth constant, the rotational speed n of the tool spindle must be adapted to the feed rate to maintain a constant feed per tooth. Hence, to fully define the requirements for speed control, the kinematics for micro milling a groove with a rounded corner are described in dependence of the feed rate. The feed per tooth f_z is defined as the ratio between the feed rate v_f and the product of the spindle rotational speed n and the number of cutting edges z:

$$f_z = \frac{v_f}{n \cdot z} \tag{1}$$

The milling path is divided into five regions, as shown in Figure 2a). The corresponding feed rate of the feed axis to maintain a constant feed per tooth (equation (1)) is shown in Figure 2b).

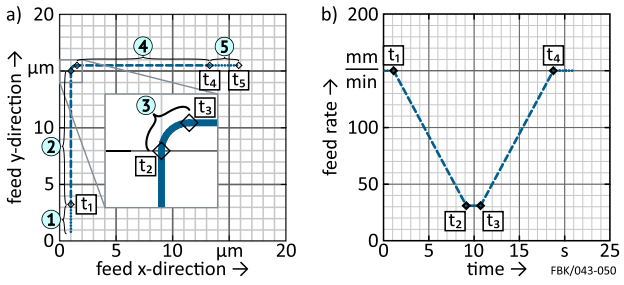

Figure 2. a) trajectory of a groove with rounded corner and b) corresponding change of feed rate

Regions 1 and 5 have a constant feed rate $v_{f,0}$ (up to t_1 and t_5 respectively), derived from the optimal feed per tooth and initial spindle speed n_0. Regions 2 and 4 reduce the feed rate (up to t_2 and t_4 respectively) to a reduced value $v_{f,red}$ before the transition area to lessen the demands on response time of the speed control. The feed rate decreases linearly in these regions when assuming maximum acceleration. Region 3 describes the transition area, where the feed rate is the lowest (up to t_3).

2.3. Feedback loop

For the control system, the overall dynamics of the plant must be modelled in the feedback loop. This includes the rotor's angular dynamics, start-up dynamics of the inlet valve, the cutting torque, and the mass-flow-rate-speed-torque characteristics of the turbine. Herein, instead of the full fluid dynamics model of the turbine, the lookup tables featuring the turbine's characteristics were implemented in the feedback loop to avoid a time-consuming recomputation during every simulation step. The mass-flow-rate-speed-torque characteristics of the turbine were limited to a maximum value corresponding to a maximum pressure of 8 bar at the valve/inlet of the turbine. A dynamic torque equilibrium was established for the rotor, considering the resultant angular acceleration due to the applied turbine torque. Additionally, frictional torque of the rotor's bearings is calculated based on fluid shear forces as presented in [9]. The resulting differential equation from the dynamic torque equilibrium can be converted into a state-space representation. Here, the rotor's angular velocity is the state vector **x**(t), turbine torque is the input vector u(t), and angular velocity is the output vector y(t). The state-space representation simplifies the differential equation by reducing its order through substitution to a first-order linear differential equation, eliminating the need for linearization. The state-space representation (the rotor's inertia included in **A** and the input matrix **B** and the frictional torque of the bearings included in the the state matrix **A**) is given in equation (2), the required input parameters are given in Table 1.

$$\begin{aligned} &\dot{\boldsymbol{x}}(t) = \boldsymbol{A}\boldsymbol{x}(t) + \boldsymbol{b}u(t), \quad y(t) = \boldsymbol{c}^T\boldsymbol{x}(t) + du(t) \\ &\boldsymbol{x}(0) = \boldsymbol{x_0}, \quad \boldsymbol{x}(t) = \omega_R, \quad u(t) = M_T, \quad y(t) = \omega_R \\ &\boldsymbol{A} = -\frac{\mu_A \cdot 2\pi \cdot R_i^3 \cdot l_{ra}}{J_z \cdot h_{ra}} - \frac{\mu_L \cdot \pi \cdot (R_o^4 - R_i^4)}{2 \cdot J_z \cdot h_{ax}} \\ &\boldsymbol{b} = 1/J_Z;\ \boldsymbol{c}^T = 1;\ d = 0;\ \boldsymbol{x_0} = n_{max} \cdot \pi/30 \end{aligned} \tag{2}$$

Table 1. Input parameters required for modelling and simulation

parameter	value
dynamic viscosity of air μ_A	18 µPa·s
inner radius of rotor R_i	10.5 mm
outer radius of rotor R_o	19 mm
length of radial bearing l_{ra}	67 mm
mass moment of inertia in z-direction J_z	185,4 g·cm²
air gap height of radial bearing h_{ra}	21.5 µm
air gap height of axial bearing h_{ax}	25 µm
intended maximum rotational speed n_{max}	125,000 min^{-1}

The start-up dynamics of the inlet valve can be modelled as part of the feedback loop or be considered during the controller design. However, the valve's fast rise times make it unsuitable for controller design, as its impact is brief and would increase controller complexity. Hence, the start-up dynamics of the inlet valve are considered as a disturbance input in the feedback loop.

The cutting torque was also modelled as a disturbance input in the closed-loop model. The cutting force was simplified as a sinusoidally oscillating force with zero crossings instead of negative values. An amplitude of 0.2 N and a tool radius of 25 µm was assumed, adopted from previous works [10]. The sinusoidal frequency was based on spindle speed.

2.4. Controller design

The desired control behaviour for the process variable (actual value of speed) was specified to follow the setpoint value (setpoint speed). A second-order (PT2) response was sought for stability, characterized by simple and stable control with a short

settling time and minimal overshoot. For this, a PIT1 compensation controller was designed using the root locus method. The PIT1 controller inherently has an integrator pole at zero, a system pole defined by the plant, and another adjustable pole and root. Parameters were chosen to ensure a PT2 response for the closed-loop system, offering a short settling time with minimal overshoot: Initially, the gain factor was set for the desired settling time, and then the rightmost pole was shifted along the real axis. Using the Controller System Designer App[1] in MATLAB[1] to determine parameters for the adjustable pole and root through linear regression results in the equation for the controller:

$$G_R(s) = 0{,}045 \cdot \frac{1 + \frac{0{,}02}{s}}{s + 100} \qquad (3)$$

To enable fast speed adjustments, a feedforward control was added. This anticipates the setpoint value, reducing control error. The feedforward control consists of the inverse model of the plant, multiplied by a PT1 element. The feedforward time of the PT1 element is an adjustable parameter and was iteratively set to 20 s, offering good control behaviour without introducing additional oscillatory behaviour. The derived equation for the feedforward control is:

$$G_{VS}^{real}(s) = \left(\frac{53940}{s + 0{,}03713}\right)^{-1} \cdot \frac{1}{1 + 20 \cdot s} \qquad (4)$$

The complete closed-loop model was set up in Simulink[1], as shown in Figure 3. It includes feedforward control (green, solid lines), the controller (red, dashed lines), and the plant (yellow, dotted lines), consisting of the turbine's mass-flow-rate-speed-torque characteristics, the rotor's angular dynamics, start-up dynamics of the inlet valve, and the cutting torque (see section 2.3). The setpoint speed was calculated corresponding to the change of the feed rate during the manufacture of a groove with constant feed per tooth (see Section 2.2 and Figure 2).

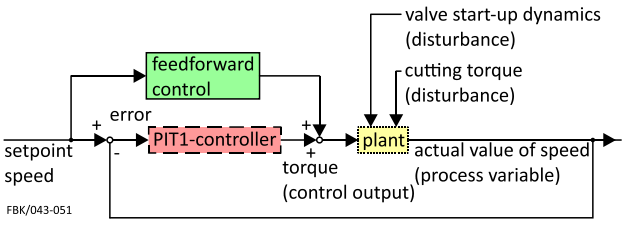

Figure 3. Schematic view of the modelled feedback loop with feedforward control

3. Results

This section examines how well the control requirements (see section 2.1) are met and how the maximum mass flow rate and torque affect the speed control. The results (Figure 4 to 6) include a numbering of regions (1 to 5), as outlined in the modelling of the milling path and feed rate in Section 2.2 and Figure 2.

3.1. Test with unlimited mass flow rate and torque

To evaluate the performance of the developed controller (equation (3)) and the feedforward control (equation (4)), the controller's transient response under ideal conditions is examined with a time-varying setpoint, without limits of the mass flow rate and torque imposed by the turbine drive. Figure 4 shows the behaviour of the setpoint value (setpoint speed) and the process variable (actual value of speed) during adjustments of the rotational speed as required to machine the described grooves with constant feed per tooth (see section 2.2 and Figure 2). The results show that the combination of controller and feedforward control provides fast and accurate speed adjustment. Further, there is no oscillatory characteristic of the process variable, the rise and settling times are very low, and the process variable converges without steady-state error. By deliberately omitting a derivative term (D-term) in the controller, the high-frequency signal of the cutting force is not amplified further and has a negligible influence on the process variable.

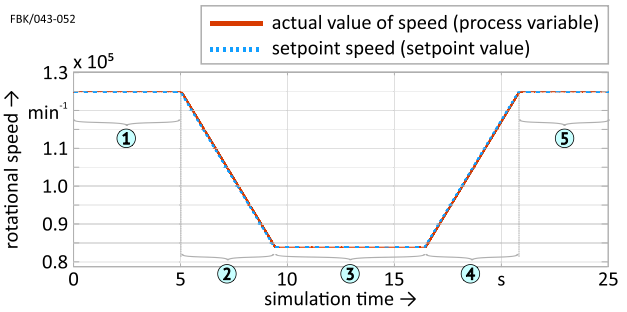

Figure 4. Behaviour of the setpoint value (setpoint speed) and the process variable (actual value of speed) during adjustments of the rotational speed with unlimited mass flow rate and torque

3.2. Test with maximum mass flow rate and torque

The control input (mass flow rate) of the control loop is limited by the maximum possible mass flow rate, which is determined by the mass throughput through the inlet valve, inlet nozzle and the geometry of the turbine. This subsequently limits the control output (torque). Figure 5 shows the additional influence on the control output and the process variable (actual value of speed) due to the maximum achievable turbine torque.

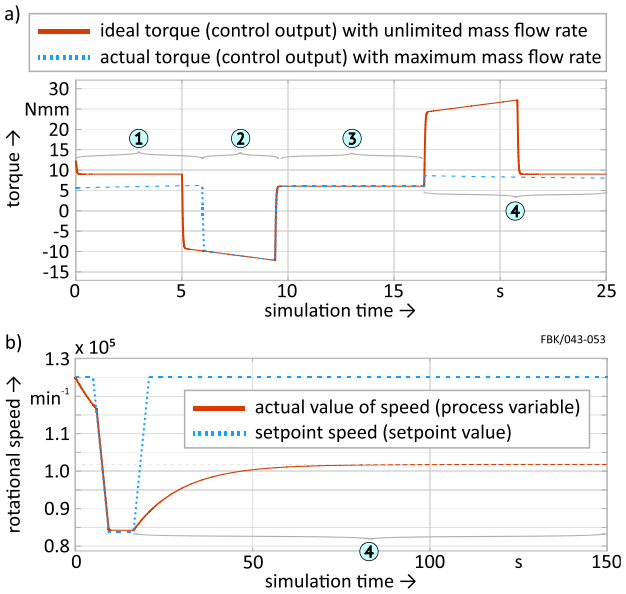

Figure 5. a) control output (torque) during adjustments of the rotational speed with maximum mass flow rate and torque and b) setpoint value (setpoint speed) and process variable (actual value of speed)

Figure 5a) shows that the achieved torque is lower than the required ideal torque, which also leads to torque having to be applied for a longer time (as seen by the longer required simulation time (150 s) to achieve a steady-state behaviour in Figure 5b)). This leads to the process variable no longer being able to match the setpoint value, as the available torque is not suffi-

cient to control the speed sufficiently quickly and reach the target speed, as Figure 5b) shows. This is reflected in an increased rise and settling time, an overshoot, and a steady-state error.

3.3. Test with artificially increased mass flow rate and torque

For further assessment of the controller, in this section an artificially increased maximum mass flow rate of 0.005 kg/s is assumed, which is higher than the actual possible mass flow rate (approx. 0.002 kg/s). The new transient response resulting from the higher maximum mass flow rate is shown in Figure 6a). This new transient response only exhibits a slight overshoot that converges slowly (as seen by the longer required simulation time (150 s) to achieve a steady-state behaviour in Figure 6a)). This is again a consequence of the maximum mass flow rate. The overshoot characteristics can be improved with further increase of mass flow rate and thus torque.

The feed per tooth can be calculated (using equation (1)) and compared for the two cases without and with speed control, as seen in Figure 6b). Due to the limited mass flow rate and thus low torque, constant feed per tooth is not achieved, even when speed control is used. Due to the controller and feedback loop, the speed adjustment leads to an increase in the feed per tooth. This increase is smaller than the reduction of the feed per tooth when no speed control is used (blue dotted lines in Figure 6b)). The small increase in feed per tooth may be better suited for machining applications, because lowering the feed per tooth can cause the minimum chip thickness to be undercut. This is not the case for a small increased feed per tooth. In that case, the optimal value for the feed per tooth is not reached for a short time and the wear of the micro milling tool is increased for the period.

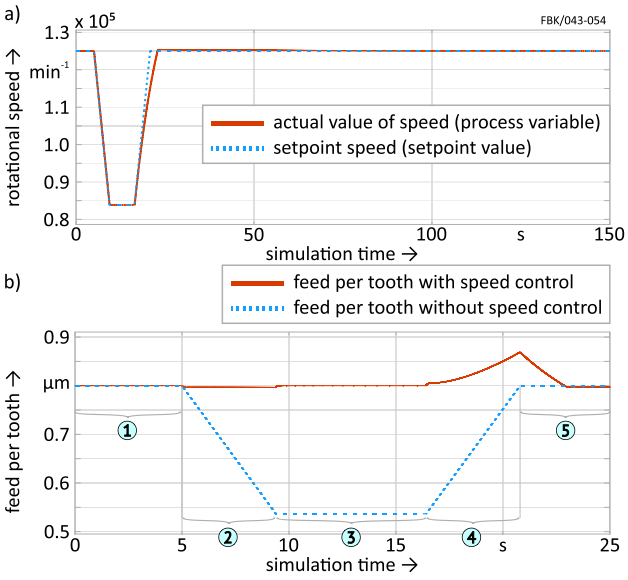

Figure 6. a) setpoint value (setpoint speed) and process variable (actual value of speed) and b) feed per tooth during adjustments of the rotational speed with artificially increased mass flow rate and torque

4. Conclusion

In this study, a control system for the speed control of a spindle's turbine drive was developed. For this purpose, a fluid dynamics model of the turbine was set up to determine the dependence between mass flow rate, rotational speed, and torque. The resulting characteristics were then stored in the form of lookup tables. The speed control was modelled as a controller in a feedback loop with feedforward control for fast adaptation and accurate control of model uncertainties and disturbances such as cutting torque. The following conclusions can be drawn:

- Tests with unlimited mass flow rate and torque show that effective speed control is possible with the devised controller and feedback loop.
- Tests with the actual possible mass flow rate and torque show that the turbine's power output is too low to adapt the spindle speed sufficiently quickly and to reach the target speed. Thus, while the presented control system is suitable, the modelled turbine is not feasible for the required speed control to enable constant feed per tooth.
- Tests with artificially increased mass flow rate show how much torque of the turbine is necessary to enable efficient speed control. Based on this, the turbine can be optimised towards a defined torque and thus required target mass flow rate and pressure at the inlet.

In future works, necessary turbine optimisations to increase the torque will be investigated to evaluate if the required inlet mass flow rate and pressure is feasible. Additionally, the turbine diameter can be increased. However, the increased moment of inertia of the rotor and the low efficiency of turbine drives in high-frequency spindles compared to electric motors must be considered.

Acknowledgement

This research was funded by the Deutsche Forschungsgemeinschaft (DFG, German Research Foundation) – project numbers 491400536.

[1]Naming of specific manufacturers is done solely for the sake of completeness and does not necessarily imply an endorsement of the named companies nor that the products are necessarily the best for the purpose.

References

[1] Chae J, Park S S, Freiheit T 2006 Investigation of micro-cutting operations. *International Journal of Machine Tools and Manufacture*

[2] Balázs B Z, Geier N, Takács M, Davim J 2020 A review on micro-milling: recent advances and future trends. *The International Journal of Advanced Manufacturing Technology*

[3] Vavruska P, Bartos F, Pesice M 2023 Effective feed rate control to maintain constant feed per tooth along toolpaths for milling complex–shaped parts. *International Journal of Advanced Manufacturing Technology* **128** 3215–3232

[4] Abele E, Altintas Y, Brecher C 2010 Machine tool spindle units. *CIRP Annals* 59 **2** 781-801

[5] Kim T, Kim K T, Hwang S, Lee S, Park N G 2001 Analysis of radial runout for symmetric and asymmetric HDD spindle motors with rotor eccentricity. *Journal of Magnetism and Magnetic Materials* 226 1232-1234.

[6] Gao Q, Chen W, Lu L, Huo D, Cheng K 2019 Aerostatic bearings design and analysis with the application to precision engineering: State-of-the-art and future perspectives. *Tribology International*

[7] Li W, Zhou Z X, Huang X M, He Z J, Du Y 2014 Development of a High-Speed and Precision Micro-Spindle for Micro-Cutting. *International Journal of Precision Engineering and Manufacturing* **15** 2375-2383

[8] Müller C, Kirsch B, Aurich J C 2017 Compact Air Bearing Spindles for Desktop Sized Machine Tools. In: Wulfsberg J, Sanders A. (eds) Small Machine Tools for Small Workpieces. *Lecture Notes in Production Engineering* 21-34

[9] Powell J W 1970 The design of aerostatic bearings. The Machinery Publishing Co. Ltd

[10] Kieren-Ehses S, Bohley M, Mayer T, Kirsch B, Aurich J C 2020 Effect of high spindle speeds on micro end milling of commercially pure titanium. *Proceedings of the 20th euspen International Conference* 63-66